NeuroImage: Clinical 19 (2018) 652–660

Contents lists available at ScienceDirect

NeuroImage: Clinical

journal homepage: www.elsevier.com/locate/ynicl

Investigation of serotonergic Parkinson's disease-related covariance pattern using [^{11}C]-DASB/PET

Jessie Fanglu Fu[a,*], Ivan Klyuzhin[b], Shuying Liu[d], Elham Shahinfard[c], Nasim Vafai[c], Jessamyn McKenzie[c], Nicole Neilson[c], Rostom Mabrouk[a], Matthew A. Sacheli[c], Daryl Wile[e], Martin J. McKeown[c], A. Jon Stoessl[c], Vesna Sossi[a]

[a] Department of Physics and Astronomy, University of British Columbia, Vancouver, BC, Canada
[b] Division of Neurology, Department of Medicine, University of British Columbia, Vancouver, BC, Canada
[c] Djavad Mowafaghian Centre for Brain Health, Pacific Parkinson's Research Centre, University of British Columbia & Vancouver Coastal Health, Vancouver, BC, Canada
[d] Department of Neurobiology, Neurology and Geriatrics, Xuanwu Hospital Capital Medical University, Beijing, China
[e] University of British Columbia, Okanagan Southern Medical Program, Kelowna, BC, Canada

ABSTRACT

We used positron emission tomography imaging with [^{11}C]-3-amino-4-(2-dimethylaminomethylphenylsulfanyl)-benzonitrile (DASB) and principal component analysis to investigate whether a specific Parkinson's disease (PD)-related spatial covariance pattern could be identified for the serotonergic system. We also explored if non-manifesting leucine-rich repeat kinase 2 (LRRK2) mutation carriers, with normal striatal dopaminergic innervation as measured with [^{11}C]-dihydrotetrabenazine (DTBZ), exhibit a distinct spatial covariance pattern compared to healthy controls and subjects with manifest PD. 15 subjects with sporadic PD, eight subjects with LRRK2 mutation-associated PD, nine LRRK2 non-manifesting mutation carriers, and nine healthy controls participated in the study. The analysis was applied to the DASB non-displaceable binding potential values evaluated in 42 pre-defined regions of interest. PD was found to be associated with a specific spatial covariance pattern, comprising relatively decreased DASB binding in the caudate, putamen and substantia nigra and relatively preserved binding in the hypothalamus and hippocampus; the expression of this pattern in PD subjects was significantly higher than in healthy controls ($P < 0.001$) and correlated significantly with disease duration ($P < 0.01$) and with DTBZ binding in the more affected putamen ($P < 0.01$). The LRRK2 non-manifesting mutation carriers expressed a different pattern, also significantly different from healthy controls ($P < 0.001$), comprising relatively decreased DASB binding in the pons, pedunculopontine nucleus, thalamus and rostral raphe nucleus, and with relatively preserved binding in the hypothalamus, amygdala, hippocampus and substantia nigra. This pattern was not present in either sporadic or LRRK2 mutation-associated PD subjects. These findings, although obtained with a relatively limited number of subjects, suggest that specific and overall distinct spatial serotonergic patterns may be associated with PD and LRRK2 mutations. Alterations in regions where relative upregulation is observed in both patterns may be indicative of compensatory mechanisms preceding or protecting from disease manifestation.

1. Introduction

Parkinson's disease (PD) is the second most frequent progressive neurodegenerative disorder (de Lau and Breteler, 2006). The cardinal features are motor deficits, including tremor, rigidity and bradykinesia, traditionally associated with dopaminergic denervation in the substantia nigra (Stoessl et al., 2012). There is however increased recognition of the importance of the disease-induced non-motor symptoms. Some of these non-motor abnormalities, including autonomic dysfunction, sleep disturbance, cognitive impairment and depression, can precede the motor deficits by years or even decades (Schrag et al., 2015). The bases for these non-motor deficits are still unclear, but it is suggested that many of them may be associated with alterations of non-dopaminergic neurotransmitter systems (Stoessl, 2009). In particular, several *in-vivo* and post-mortem studies support the hypothesis that progressive alterations of the serotonergic system may contribute to a number of such non-motor alterations (Politis and Loane, 2011). A large body of evidence has indeed been gathered from *in-vivo* PET studies

* Corresponding author at: F143-2211 Wesbrook Mall, Vancouver, BC V6T 2B5, Canada.
E-mail address: jfu@phas.ubc.ca (J.F. Fu).

https://doi.org/10.1016/j.nicl.2018.05.022
Received 12 January 2018; Received in revised form 1 May 2018; Accepted 19 May 2018
Available online 21 May 2018

using the radioligand [^{11}C]-3-amino-4- (2-dimethylaminomethylphenylsulfany1)-benzonitrile (DASB) which binds to the serotonin transporter (SERT). Reduced DASB binding in the caudate, thalamus, hypothalamus and anterior cingulate cortex has been observed in early disease (< 5 years of disease duration), and additional reductions in the putamen, insula, posterior cingulate cortex and prefrontal cortex have been detected in mild disease (5–10 years of disease duration). Ventral striatum, raphe nuclei and amygdala were only affected in advanced disease (> 10 years of disease duration) (Politis et al., 2010a, 2010b). Reduction in DASB binding in the caudate, putamen and raphe nuclei also significantly correlated with tremor severity on posture and action (Loane et al., 2013). Studies have suggested PD subjects experiencing non-motor deficits showed upregulated DASB binding in some brain regions compared to subjects without such deficit. In particular, PD subjects with abnormal Body Mass Index (BMI) alterations had significantly increased DASB binding in the raphe nuclei, hypothalamus, caudate and ventral striatum (Politis et al., 2011). PD subjects with depressive symptoms had significantly increased DASB binding in the amygdala, hypothalamus, caudal raphe nuclei, and posterior cingulate cortex compared to matched-PD patients without depressive symptomatology but not compared to healthy controls (Politis and Loane, 2011).

In addition to its relevance to manifest PD, alterations of the serotonergic system are deemed to play a role in the presymptomatic or non-motor stage of the disease. According to Braak staging of PD pathology, Lewy body and neurite deposition occur within the raphe nuclei at stage two, whereas midbrain, substantia nigra, amygdala and hypothalamus, more closely linked to the dopaminergic system, are affected at stage three before the onset of motor deficits (Braak et al., 2003, 2004). The serotonergic system is thus hypothesized to be affected by disease prior to the dopaminergic system and play a significant role in premotor deficits. Despite the likelihood of non-motor deficits preceding motor impairment, the investigation of prodromal abnormalities is inherently difficult; non-motor deficits are not highly specific for PD and the disease diagnosis is currently based solely on the characteristic motor features. However, investigating subjects at a higher risk of PD, such as carriers of specific genetic mutations, might provide some insights into the prodromal stage of the disease. In this context, it is important to investigate mutation carriers in both, the asymptomatic and the symptomatic stages, to enable inference about the relevance of the alternations observed in the mutation carriers to those observed in sporadic PD (sPD) and the progression of such alterations. While several mutations are known to increase the risk of PD, in this work we concentrate on the mutation in the leucine-rich repeat kinase 2 (LRKK2).

Mutations in the LRRK2 gene are the most common genetic risk factors for autosomal dominantly-inherited PD, and the most common mutation of the LRRK2 gene is G2019S. The prevalence of LRRK2 G2019S mutation is approximately 4% in familial cases and 1% in sporadic cases (Bardien et al., 2011; Healy et al., 2008). The risk for non-manifesting LRRK2 mutation carriers (LRRK2-NMC) to develop overt disease is 28% at age 59 years, 51% at 69 years and 74% at 79 years (Healy et al., 2008); however, the estimated disease penetrance varies widely depending on age, ethnic group and genetic and environmental modifiers (Marder et al., 2015; Trinh et al., 2016). It is now commonly accepted that sPD and LRRK2 mutation carriers with manifest PD (LRRK2-PD) show similar patterns of presynaptic dopaminergic degeneration (Adams et al., 2005; Marras et al., 2011, 2016; Nandhagopal et al., 2008). Further, LRRK2-NMC subjects have been found to have lower dopamine transporter density (Nandhagopal et al., 2008) and increased dopamine turnover (Sossi et al., 2010). From the clinical point of view sPD and LRRK2-PD are for the most part similar, albeit some differences are observed: LRRK2-PD is typically associated with a lower non-motor symptom burden prior to the onset of overt disease and slower progression of motor deficits once disease becomes manifest (Healy et al., 2008; Marras et al., 2016; Sierra et al., 2013; Srivatsal et al., 2015). Likewise, LRRK2-PD is generally associated with a lower frequency of cognitive impairment (Srivatsal et al., 2015). Taken together, these findings may point towards the existence of some mutation-related compensatory mechanisms that either protect from disease occurrence or positively influence disease progression. In this context we have recently found that LRRK2-NMC subjects present increased SERT density compared to healthy controls in the hypothalamus (Wile et al., 2017) and significantly increased cholinergic activity in the cortical regions (Liu et al., 2018). In light of the demonstrated relevance of the serotonergic system to PD evolution and progression, further analysis of the imaging data is warranted. In particular, it may be informative to explore if alteration of the serotonergic system follows distinct spatial patterns or networks, relating to its widespread projections from the raphe nuclei. In addition to providing novel information, pattern analysis may be more sensitive to disease-related effects for SERT imaging data compared to localized changes which are generally explored with univariate analyses.

Network-based analyses have the capacity to provide additional and complementary information to that achieved by standard univariate analyses alone; multivariate pattern analyses evaluate the covariance of tracer binding between multiple brain regions, and thus can provide insight into the interactions between multiple regions with a common projection source in addition to mean differences between groups (Habeck et al., 2010). Pattern analysis also affords stronger statistical power by reducing the need for stringent and sometimes overly conservative multiple comparison corrections. Several multivariate pattern analysis methods have been used to explore functional networks using PET imaging, mostly focusing on metabolic patterns assessed with [^{18}F]-fluorodeoxyglucose (FDG) (Eidelberg, 2009). Disease-specific spatial covariance patterns were investigated using principal component analysis (PCA). Using a PCA-based scaled subprofile model (SSM), a Parkinson's disease-related pattern (PDRP) derived from FDG was found to accurately discriminate PD subjects from healthy controls. This PDRP was characterized by increased pallidothalamic and pontine activity associated with relatively reduced activity in prefrontal and parietal cortex. It was also found to correlate consistently with Unified Parkinson's Disease Rating Scale (UPDRS) motor scores (Eidelberg, 2009), clinical response to therapy (Eckert et al., 2007), and bradykinesia and executive dysfunction (Lozza et al., 2004). SSM has also been applied to identify the Parkinson's disease-related cognitive pattern (PDCP), also with FDG PET, characterized by relatively increased activity in the cerebellar vermis and dentate nuclei with associated reduced activity in frontal and parietal association areas (Huang et al., 2007). Even though the SSM method is a well-documented method, it has not been previously applied to neurotransmitter systems in PET.

In this work we use the SSM method to investigate if (i) there is a PD specific alteration of the functional SERT network across selected brain regions, where relevance to PD is additionally tested by relating pattern expression to clinical scores and dopaminergic denervation as measured by striatal [^{11}C]-dihydrotetrabenazine (DTBZ, a marker for the vesicular monoamine transporter 2 (VMAT2)) binding; (ii) LRRK2-PD is characterized by the same pattern; (iii) LRRK2-NMC subjects express a similar or different pattern. SSM with cross validation was first applied to [^{11}C]-DASB PET data of sPD subjects; upon definition of the serotonergic Parkinson's disease-related pattern (SPDRP) the strength of its expression was evaluated in the LRRK2-PD and LRRK2-NMC groups. While in LRRK2-PD, expression of this pattern would indicate similar overall disease-related alterations, the presence of such a pattern in the LRRK2-NMC could be taken to reflect similar dysfunction of the serotonergic system during the prodromal phase of disease, or an increased risk of or propensity to disease. The presence of a different LRRK2-NMC spatial covariance pattern would suggest either compensatory or genotype specific alterations. The analysis included imaging data used for the univariate analysis describe in previous publication (Wile et al., 2017). Finally, in order to check for consistency between this more extended analysis and our first results presented in Wile et al.,

Table 1
Characteristics of study participants.

	Healthy control (n = 9)	sPD (n = 15)	LRRK2-PD (n = 8)	LRRK2-NMC (n = 9)	Global p-Value	p-Value for sPD vs LRRK2-PD	p-Value for sPD vs LRRK2-NMC	p-Value for LRRK2-NMC vs HC
Gender ratio (male:female)	6:3	9:6	3:5	4:5	N/A	0.4	0.675	0.637
Age (years)	56 ± 14	59 ± 8	66 ± 15	50 ± 11	0.176	0.785	0.39	0.591
Disease duration (years)[§]		3.4 ± 2.7	7.4 ± 5.0		N/A	0.058	N/A	N/A
MDS-UPDRS part III score		16 ± 7	22 ± 10		N/A	0.248	N/A	N/A
Hoehn and Yahr stage		1.6 ± 0.5	2 ± 1.1		N/A	0.145	N/A	N/A
Montreal cognitive assessment score (MoCA)[†]		28.0 ± 1.5	26.3 ± 2.2	27.7 ± 2.3	0.2	0.313	0.743	N/A
Beck depression inventory (BDI)[‡]		4.4 ± 3.5	9 ± 6.8	4.7 ± 2.7	0.117	0.104	0.975	N/A
Number of participants with specific mutations			6 G2019S/2 R1441C	9 G2019S	N/A	0.206	N/A	N/A

Data are mean ± standard deviation, unless otherwise indicated. sPD = sporadic Parkinson's disease subjects; LRRK2-PD = manifest LRRK2 mutation carriers; LRRK2-NMC = non-manifesting LRRK2 mutation carriers; MDS-UPDRS = Movement Disorder Society Unified Parkinson's Disease Rating Scale; N/A = not applicable.

[§] Disease duration was estimated as time from onset of motor symptoms as reported by the patients.

[†] Data from 8 of 9 healthy controls, 15 of 15 sPD, 5 of 8 LRRK2-PD, and 4 of 9 LRRK2-NMC (missing information was due to language barriers).

[‡] Data from 15 of 15 sPD, 5 of 8 LRRK2-PD, and 6 of 9 LRRK2-NMC.

we applied complementary univariate analyses to regions which were found to be significantly involved in the SPDRP and LRRK2-NMC patterns. The same DTBZ binding data as reported in Wile et al. (2017) were used.

2. Materials and methods

2.1. Study participants

The study included 15 sPD, eight LRRK2-PD, nine LRRK2-NMC, and nine healthy controls age-matched to both sPD and LRRK2-PD groups (Table 1); two additional sPD and one additional LRRK2-PD subjects compared to Wile et al. Exclusion criteria included clinical history of depression, active anti-depressant therapy or medication with known serotonergic action and a BMI > 35. The healthy controls had no history of neurological or psychiatric disorders and were not taking any medication. Disease duration was estimated as time from onset of motor symptoms as reported by the subjects. The PD subjects were clinically evaluated with the Movement Disorder Society Unified Parkinson's Disease Rating Scale part III (MDS-UPDRS-III) and Hoehn and Yahr scale (H&Y) to assess motor dysfunctions, Montreal Cognitive Assessment (MoCA) scores to assess cognitive performance and Beck Depression Inventory (BDI). All assessments were performed off medication. The study was approved by the Clinical Research Ethics Board of the University of British Columbia and all subjects provided written informed consents.

2.2. Statistical analysis on clinical data

We compared age, MoCA and BDI scores between subject groups using analysis of variance (ANOVA) followed by post-hoc analyses using Tukey's Honestly Significant Differences Procedure. We assessed gender as a binomial variable with Fisher's exact test. We ascertained differences in disease duration and MDS-UPDRS-III between sPD and LRRK2-PD subjects by the independent two-tailed t-test. H&Y scores were compared between sPD and LRRK2-PD subjects using Mann-Whitney test. All P-values were false discovery rate-corrected for multiple comparisons.

2.3. Scanning protocol

All study participants underwent a [^{11}C]-DASB PET scan and a T1-weighted brain Magnetic Resonance Imaging (MRI) scan. Prior to PET imaging, patients withdrew from all anti-parkinsonian medications for at least 12 h. 558 + 2 MBq of [^{11}C]-DASB were administered by intravenous injection over 60 s using an infusion pump (Harvard Instruments). Participants were positioned using external lasers aligning the gantry with the inferior orbital-external meatal line, and custom fitted thermoplastic masks were applied to minimize head movement. All patients were scanned on a Siemens High Resolution Research Tomograph (HRRT, Knoxville, TN) with a spatial resolution of (2.5 mm)^3 (de Jong et al., 2007). Acquired data were binned into 18 time frames (frame duration: 4 × 60 s, 3 × 120 s, 8 × 300 s, 3 × 600 s; image dimension = 256 × 256 × 207; voxel size = (1.22 mm)^3) for a total duration of 80 min. Transmission scans required for attenuation correction were performed over ten minutes with a rotating ^{137}Cs source. PET images were reconstructed using the 3D list-mode ordinary Poisson Ordered Subset Expectation Maximization (OP-OSEM) algorithm (Comtat et al., 2004) with 16 subsets and six iterations, with corrections for decay, dead-time, normalization, attenuation, scattered and random coincidences. After reconstruction, the images were smoothed with a 3.0-mm full-width at half maximum (FWHM) Gaussian filter to reduce noise. The frames were spatially realigned for each subject with rigid-body transformation to minimize the impact of motion artifacts during scans. The structural MRI scans were performed on a Philips Achieva 3.0T MRI scanner (Phillips Healthcare, Best, NL) using the T1 turbo field echo (TFE) sequence (TR/TE = 7.7/3.6 ms; TFE shots = 218; flip angle = 8 degrees; image dimension: 256 × 256 × 170; voxel size (1 mm)^3). sPD subjects and LRRK2 mutation carriers also underwent an additional DTBZ PET scan to obtain complementary information on the dopaminergic integrity. Scanning protocol, imaging processing steps and results of the analysis of DTBZ data were previously reported (Wile et al., 2017).

2.4. Image processing and analysis

Image preprocessing was done using Statistical Parametric Mapping (SPM12) software (Wellcome Department of Cognitive Neurology, University College London, UK) running on Matlab 9.0 (Mathworks Inc., Natick, MA) and MEDx (Sensor Systems, Sterling, VA). The MRI images were resampled with trilinear interpolation to match the voxel size of the PET images. The resized MRI images were then coregistered to the corresponding mean PET images (mean of 18 frames) using normalized mutual information to estimate the affine transformation for each subject. These resized MRI images were then warped into the Montreal Neurological Institute (MNI) space and their inverse

deformation fields were saved. The inverse deformation field vectors were applied to region-of-interest (ROI) templates predefined in the MNI space to bring them into the individual subject's PET space in a single step. The quality of each processing step was visually checked for all scans.

The ROI templates were defined by experienced neurologists in the MNI space using MRI and PET data from healthy subjects for a total of 43 non-overlapping ROIs which are known to be involved in the serotonergic system. The regions included medulla, dorsal midbrain, pons, rostral raphe nucleus, ventral tegmental area and 19 ROIs placed bilaterally (resulting in 38 ROIs over both hemispheres): anterior and posterior cingulate, amygdala, caudate, cerebellum, dorsolateral prefrontal cortex, hypothalamus, insula, orbital frontal cortex, pedunculopontine nucleus (PPN), putamen (anterior, middle and posterior), substantia nigra, thalamus, ventral striatum, hippocampus, dentate nucleus, and globus pallidus. Decay-corrected time-activity curves (TACs) were calculated for each ROI using the Marsbar toolbox in SPM. Non-displaceable binding potential (BP_{ND}) (Innis et al., 2007) values in 42 ROIs were obtained using the Simplified Reference Tissue Model (SRTM) with the cerebellum as reference region (Gunn et al., 1997). ROI-based BP_{ND} values derived from SRTM were also compared with mean parametric BP_{ND} values in each ROI derived using two-step SRTM (SRTM2) (Wu and Carson, 2002). As the BP_{ND} values derived with the two methods were highly comparable, we only used the SRTM method for later analyses.

2.5. SSM multivariate pattern analysis

We applied SSM with repeated five-fold cross validation to DASB BP_{ND} data in 42 ROIs to identify disease and mutation-related spatial covariance patterns using in-house Matlab scripts. A detailed review of the mathematical principles and basic assumptions for SSM was previously published (Eidelberg, 2009). Regional DASB BP_{ND} data were first centered by subtracting subject and region means to obtain the residual profiles; this ensures that the analysis is minimally sensitive to global scaling effects. PCA then decomposes the residual profile into orthogonal spatial covariance patterns along each principal component (PC) and yields two outputs of interest for further analysis: 1) Regional weights, which are loadings for each ROI that contributes to the spatial covariance pattern along each PC and 2) PC scores, here referred to as subject scores, which quantify the expressions of the covariance patterns for each subject. To identify robust disease or mutation-related covariance patterns, the following steps were implemented:

1. Subject scores along each PC were entered as independent variables into a forward stepwise logistic regression model, using group assignments as dependent variables. To limit the number of variables, only PCs accounting for at least 5% of the total subject by region variance were entered into the regression model. The resulting covariance pattern was the linear combination of regional weights which gave the lowest Akaike Information Criterion (AIC) score (Akaike, 1976).
2. 1000 iterations of five-fold cross validation were performed. In each iteration, subjects were randomly divided into five subsets. Four subsets (80% of the data) were used to identify the covariance pattern and examine the effect of subject variation.
3. The final disease or mutation-specific covariance pattern was the average of the covariance patterns obtained from all iterations. Regional weights for this averaged covariance pattern were *Z*-transformed to determine significant regional contributions with weights greater than one ('significant weights').
4. Subject scores in all subject groups were then computed by projecting the residual profiles onto the average covariance pattern using the topographic profile rating (TPR) method (Eidelberg, 2009). Projected subject scores were also *Z*-transformed and analysis of covariance (ANCOVA) was performed to test the group discrimination power of the average covariance pattern using age as a covariate (see results).
5. Steps one to four were performed separately for sPD versus healthy controls and for LRRK2-NMC versus healthy controls.
6. Forward stepwise multiple regression analyses were performed between the projected subject scores in participants with PD and age of symptom onset, disease duration, UPDRS motor score and DTBZ binding to examine the correlations of the subject pattern expressions with clinical measurements and dopaminergic denervation.

2.6. Univariate ROI Analysis

After applying network analysis, we performed ANOVA on DASB BP_{ND} data between the left and right hemispheres and between the subject groups only for those regions that showed significant weights in the SSM multivariate pattern analysis, in order to limit the number of comparisons and to interpret the results of the SSM analysis in the context of absolute binding values. As no difference between the left and right hemispheres was identified, values from the corresponding regions in the two hemispheres were averaged to reduce the number of comparisons. Because the LRRK2-NMC subjects were slightly younger than the sPD subjects (Table 1), we also performed ANCOVA with age as a covariate when comparing these two groups. False positive rates were controlled at $P = 0.05$ using Bonferroni-Holm's step-down procedure (Holm, 1979).

3. Results

There was no significant difference in any clinical variables between subject groups.

3.1. sPD and LRRK-PD spatial covariance pattern (SPDRP)

A spatial covariance pattern (the SPDRP) was identified with significantly higher scores for sPD subjects than healthy controls ($P < 0.001$). The SPDRP was characterized by relatively decreased DASB binding in caudate, putamen and substantia nigra, and relatively increased DASB binding in hypothalamus and hippocampus (Fig.1). This pattern had the largest contributions from PC2, PC3 and PC4, which collectively accounted for 28% of the total variance. When projecting data from the LRRK2 mutation carriers onto this pattern, LRRK2-PD showed a significantly higher expression of SPDRP compared to healthy controls ($P < 0.05$) (Fig.2). Although only the sPD subject data were used to determine SPDRP, there was no significant difference between the sPD and LRRK2-PD subject scores. There was one outlier in the LRRK2-NMC group with very high SPDRP expression (H814); this subject was the youngest participant in the study (more than two standard deviations away from the mean age of this subject group). Subject H814 showed normal expression of LRRK2-NMC pattern compared to other LRRK2-NMC subjects and striatal DTBZ binding in the control range. When excluding this subject from the group comparison, there was no significant difference between LRRK2-NMC and the healthy controls, but a significant difference between LRRK2-NMC and sPD groups ($P < 0.05$).

SPDRP expression in sPD subjects correlated significantly with disease duration ($P < 0.01$) (Fig.3 left); this correlation remained significant after correcting for the age of disease onset ($P < 0.05$). Combined LRRK2-PD and sPD subject scores also correlated significantly with disease duration ($P < 0.01$) after removing two outliers (H1079 and H1013), both LRRK2-PD. One outlier (H1079), while having a disease duration of ten years and significant reduced DTBZ binding compared to age-matched controls, only scored 13 on the UPDRS motor scale, indicative of unusually slow disease progression. The second outlier (H1013) was initially found to be a subject without evidence of dopaminergic deficit (SWEDD) based on 6-[^{18}F]-fluoro-L-dopa (^{18}F-dopa) performed at the time of diagnosis and later developed

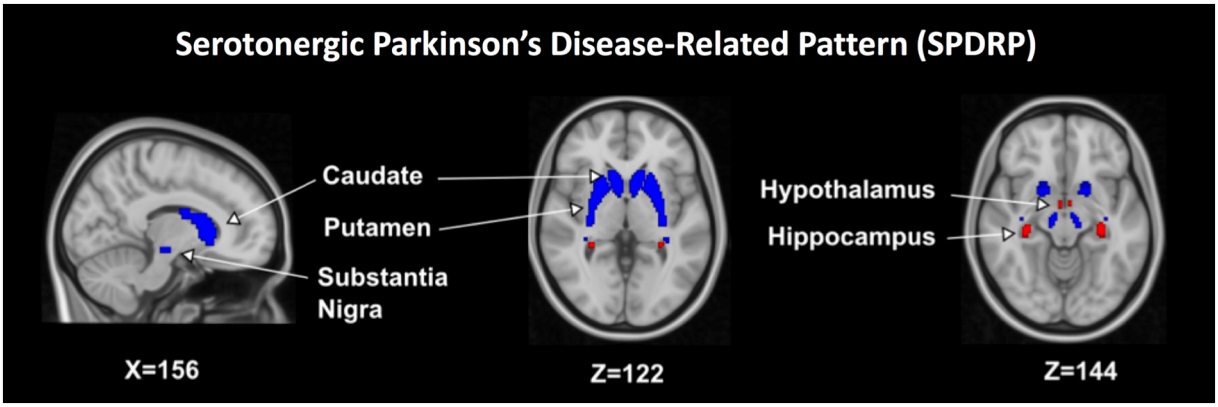

Fig. 1. Serotonergic Parkinson's disease-related pattern (SPDRP) identified by comparing sporadic Parkinson's disease subjects and healthy controls. Regions with significant weights on the averaged SPDRP were overlaid onto a T1 MRI image. Blue (red) indicates regions with relatively decreased (increased) binding in sporadic Parkinson's disease subjects compared to healthy controls. MRI = magnetic resonance imaging.

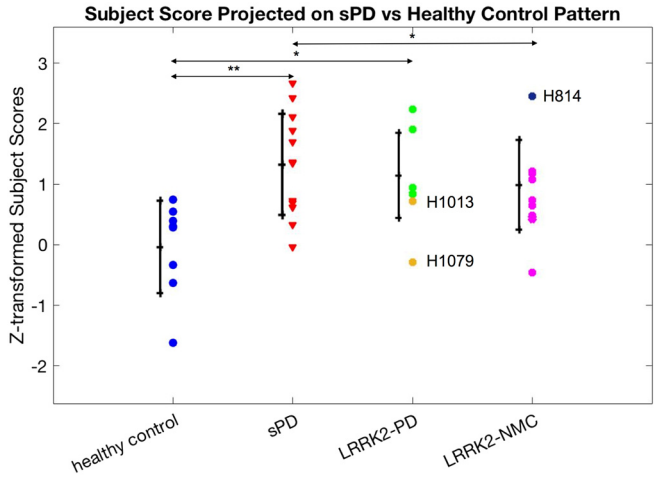

Fig. 2. Subject scores projected onto the serotonergic Parkinson's disease-related pattern (SPDPR) for all four subject groups. The three outliers were labeled as H1013 and H1079 in the LRRK2-PD group, and H814 in the LRRK2-NMC group.
sPD = sporadic Parkinson's disease subjects; LRRK2-PD = manifested LRRK2 mutation carriers; LRRK2-NMC = non-manifesting LRRK2 mutation carriers; * = significant at $P < 0.05$ level; ** = significant at $P < 0.01$ level.

unequivocal PD with bilateral striatal dopaminergic denervation and relatively preserved SERT binding in the putamen and several cortical regions (Wile et al., 2016); this subject had much longer disease duration compared to all other manifest subjects (17 years of disease duration compared to a mean of 4.2 years in all other subjects). Interestingly these two subjects showed the lowest SPDRP expression in the LRRK2-PD group (Fig.2), while their expressions of LRRK2-NMC pattern were in line with that of the other LRRK2-PD subjects. SPDRP expression did not correlate with any other clinical variables.

SPDRP expression in sPD and LRRK2-PD also correlated significantly with DTBZ binding in the more affected putamen ($P < 0.01$) (Fig.3 right). H1079 and H1013 did not appear as outliers in this correlation.

3.2. LRRK2-NMC spatial covariance pattern

A pattern along which the LRRK2-NMC subject scores were significantly higher compared to those of healthy controls ($P < 0.001$) was also identified (Fig. 4); The pattern had the largest contributions from PC2, which accounted for 10% of the total variance. The LRRK2-NMC pattern was comprised of a relatively decreased DASB binding in the pons, PPN, thalamus and raphe nucleus, and relatively increased binding in the hypothalamus, amygdala, hippocampus and substantia nigra (Fig.5). Neither sPD nor the LRRK-PD showed a significant

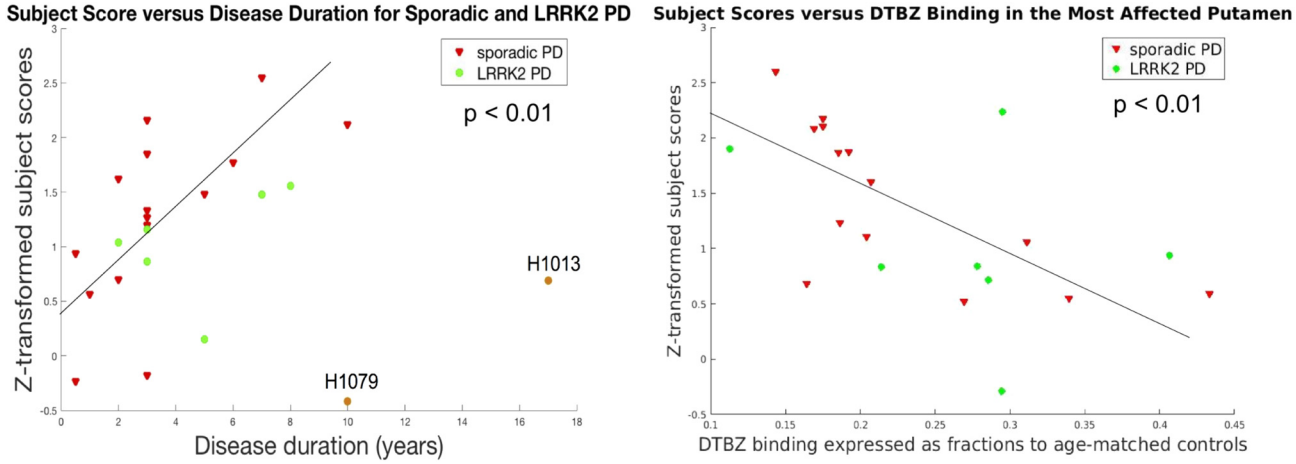

Fig. 3. Scatter plot of projected subject scores, denoting the strength of the serotonergic Parkinson's disease-related pattern (SPDRP) expression as a function of disease durations (left) and as a function of DTBZ binding expressed as fractions to age-matched normal controls (right) for sporadic PD and LRRK2-PD. The two outliers are labeled in the same way as in Fig.2. The best line fit was done without these two subjects.
PD = Parkinson's disease; LRRK2-PD = manifest LRRK2 mutation carriers.

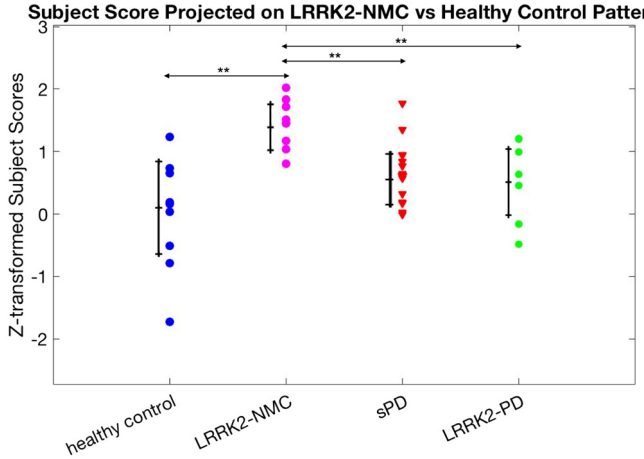

Fig. 4. Subject scores projected onto LRRK2-NMC pattern in all four subject groups.
sPD = sporadic Parkinson's disease subjects; LRRK2-PD = manifested LRRK2 mutation carriers; LRRK2-NMC = non = manifesting LRRK2 mutation carriers; ** = significant at $P < 0.01$ level.

expression of this LRRK2-NMC pattern. This pattern expression did not show correlation with any clinical measurements or DTBZ binding.

3.3. Univariate ROI analysis

Only DASB BP_{ND} values from regions significantly contributing to the spatial pattern obtained in the DASB multivariate analysis were tested in the univariate ROI analysis; they included the caudate, putamen, hypothalamus, hippocampus, amygdala, substantia nigra, thalamus, pons, PPN and raphe nucleus. There was no significant difference in DASB binding between the left and right hemispheric ROIs in any subject group, so average BP_{ND} values from both hemispheres were used to reduce the number of comparisons. There was no significant difference between LRRK2-PD and sPD in any brain region. Both sPD and LRRK2-PD showed significantly reduced DASB binding in the caudate compared to healthy controls ($P < 0.01$ for both groups), however this reduction was not significant after correcting for multiple comparisons. LRRK2-NMC showed significantly higher DASB binding compared to healthy controls in hypothalamus ($P < 0.01$) and hippocampus ($P < 0.05$). There was a significant age effect in hypothalamus ($P < 0.01$), pons ($P < 0.05$), substantia nigra ($P < 0.05$) and raphe nucleus ($P < 0.05$) in the healthy control group. With age as a covariate, LRRK2-NMC only showed significantly higher DASB binding compared to healthy controls in hypothalamus ($P < 0.05$). However, again, the significance of the results did not survive multiple comparison correction for any region. As previously reported, all LRRK2-NMC subjects showed normal DTBZ binding compared to age-matched controls except for one subject and no correlation was obtained between DASB and DTBZ binding in any individual region.

4. Discussion

Using a multivariate pattern analysis, we found a significant disease-specific pattern (SPDRP) in the sPD subjects, and LRRK2-PD subjects also showed a significant elevation of this pattern. A significant positive correlation between the strength of the SPDRP expression and disease duration was found for both manifest disease groups, with the exception of two subjects who had the lowest SPDRP expression; one presented a with an unusual (milder) motor symptom progression, while the other outlier was initially classified as a SWEDD and when imaged 17 years later exhibited bilateral striatal dopaminergic denervation with relatively preserved SERT in the putamen and several cortical regions (Wile et al., 2016). A very significant correlation between the strength of the SPDRP expression and dopaminergic deficit in the more affected putamen was also observed. In this case the two subjects described above no longer appeared outliers, which is likely suggestive of a mechanistic link between dopaminergic denervation and serotonergic connectivity. Interestingly, no correlation between DTBZ and DASB BP_{ND} values of individual regions was found suggesting PD affects the serotonergic system on a more global network level rather than any particular region in isolation. This observation also highlights the complementarity of the information provided by a network approach.

4.1. Possible functional basis for SPDRP and LRRK2-NMC pattern topography

In SPDRP, the caudate showed the most significant relative reduction in DASB binding followed by the putamen. Once disease manifests, the observed relative reductions in the striatum agree with previous findings that PD is associated with an absolute decrease in DASB binding in caudate and putamen compared to healthy controls (Kish et al., 2008; Politis and Loane, 2011). Unlike the dopaminergic system where the posterior putamen is more affected by the disease, there is a preferential loss of SERT in the caudate. Univariate analysis in this study failed to detect significant group separation in both caudate and putamen after correcting for multiple comparisons in PD subjects and LRRK-NMC compared to healthy controls. This might be due to the fact that only early PD subjects were included in this study, whereas subjects involved in other studies had a wider range of disease durations. However, the pattern analysis still accurately captured this disease effect even in an early disease stage.

Relative upregulation of DASB binding in the substantia nigra was only evident at the non-manifesting stage, as it was observed only in the LRRK2-NMC pattern; DASB binding in the substantia nigra was

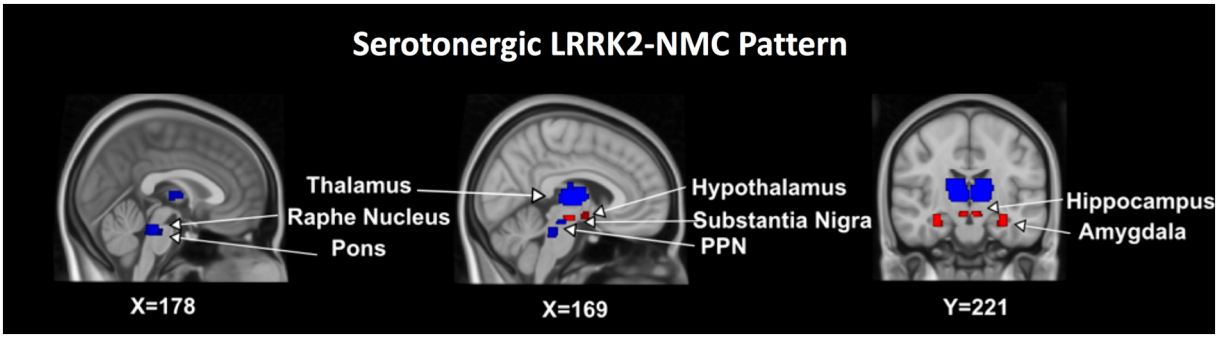

Fig. 5. Serotonergic LRRK2-NMC pattern identified by comparing LRRK2-NMC and healthy controls. Regions with significant weights on the averaged LRRK2-NMC pattern were overlaid onto a T1 MRI image. Blue (red) indicates regions with relatively decreased (increased) binding in LRRK2-NMC compared to healthy controls. LRRK2-NMC = non-manifesting LRRK2 mutation carriers; MRI = magnetic resonance imaging; PPN = pedunculopontine nucleus.

relatively reduced in subjects with manifest disease. This is consistent with the fact that disease causes more alterations in the substantia nigra compared to other regions such as the hypothalamus and hippocampus, where binding remained relatively upregulated even in the presence of disease. While dopaminergic neurons originate in the substantia nigra, 5HT neurons show highly variable densities and patterns of innervation in the basal ganglia. The substantia nigra receives the densest 5HT innervation, whereas the caudate is more heterogeneously innervated than the putamen (Scholtissen et al., 2006). The relative upregulation of DASB binding in LRRK2-NMC may indicate a compensatory or protective role of serotonergic innervation in the substantia nigra, which is no longer present once disease becomes manifest. Such upregulation could conceivably contribute to the incomplete penetrance of LRRK2 mutations.

The relative upregulation of DASB binding in the hypothalamus and hippocampus observed in the LRRK2-NMC pattern is present even after disease manifests. Upregulation of DASB binding in the hypothalamus has also been found to correlate with several aspects in PD such as depression and abnormal weight changes (Politis et al., 2010a, 2010b; Politis et al., 2011). In task-related functional MRI (fMRI) studies, the hippocampus has been shown to be preferentially activated in mild PD subjects when performing a cognitive planning task, at the expense of a reduction in the activation of the right caudate. This may indicate that hippocampal hyperactivity compensates for striatal deficiencies and thus possibly induces a shift towards the declarative memory system in response to a defect in procedural memory, which is related to the frontostriatal system (Dagher et al., 2001). While this is a reasonable interpretation for the subjects with active disease, the reason for this upregulation in the LRRK2-NMC, where the dopaminergic system is still mostly intact, is still unclear. It has been observed however, that the cholinergic system, also related to cognition, is upregulated in this patient population (Liu et al., 2018).

LRRK2-NMC pattern was also characterized by relatively reduced DASB binding in the raphe nucleus, pons, PPN and thalamus. Because there was an overall increase in absolute binding magnitudes in LRRK2-NMC compared to healthy controls, these regions were actually less upregulated compared to other regions in LRRK2-NMC, rather than reduced compared to healthy controls. The LRRK2-NMC pattern also showed relatively increased binding in the amygdala, which was not upregulated in the SPDRP. Abnormal activation of the amygdala in response to processing of fearful stimuli has been observed in early disease stage even in the absence of noticeable behavioral differences; the abnormality was partially reversed with dopamine replacement (Tessitore et al., 2002). Given that dopaminergic function in the amygdala may be reduced in PD (Ouchi et al., 1999), the relative upregulation of the serotonergic system in the asymptomatic stage may be of compensatory nature. In addition, amygdala hyperactivity in the serotonergic system in PD has also been associated with depression (Politis and Loane, 2011). Relative upregulation in amygdala in LRRK2-NMC pattern may partially explain the higher propensity to depression in LRRK2-PD compared to sPD (Marras et al., 2011).

4.2. LRRK2-NMC pattern – protection or compensation

LRRK2-NMC subjects did not show a significant expression of SPDRP, except for one subject with a clear expression of the disease pattern (H814 as shown in Fig.2), whose dopaminergic function appeared intact. LRRK2-NMC subjects however expressed a unique pattern compared to healthy controls, which may be related to mutation specific alterations, such as the established decrease in dopamine transporter binding (Adams et al., 2005; Sossi et al., 2010; Wile et al., 2017) and increase in dopamine turnover in the putamen (Sossi et al., 2010). Interestingly the two patterns showed several common regions of relative upregulation; whether such upregulation may be protective against other disease-inducing mechanisms or a risk factor for disease is still unclear at this stage. While clear alterations in other regions are observed in the SPDRP, notably a decreased DASB binding in the substantia nigra, it may be reasonable to surmise that relatively increased expression of SERT (and presumably of 5HT nerve terminals) offers some degree of protection of neurons or compensation to delay symptom manifestation since the upregulation persists after disease onset. Alternatively, an increase in DASB binding could be related to reduced SERT occupancy secondary to lower levels of 5HT neurons in the synapse (Meyer et al., 2001). Evidence for this hypothesis is however quite marginal. The spread in LRRK2-NMC subject scores onto SPDRP may reflect inherent increased risk of disease (or pre-manifest disease) in subjects with high pattern expression and the incomplete penetrance of LRRK2 mutation; most of our LRRK2-NMC subjects were younger than 59 years, the expected age of disease onset for the G2019S mutation-associated disease (Healy et al., 2008). Two LRRK2-PD subjects had R1441C mutations; however, they did not appear as outliers in either SPDRP or LRRK2-NMC pattern. All LRRK2-NMC subjects showed normal striatal dopaminergic innervation except for one outlier subject, whose serotonergic patterns strength was in line with those observed in the LRRK2-NMC group. This indicates that the changes we observed in LRRK2-NMC pattern are generally not accompanied by dopaminergic deficit and may indeed be related to protective mechanisms. Longitudinal observations which would capture subject phenoconversion would help to explain the high SPDRP expression in some of the LRRK2-NMC subjects, and the protection or compensatory role of the serotonergic system in PD.

4.3. Comparison with univariate analysis

Regions with most significant changes in DASB binding in univariate analysis also showed the most significant contributions to the patterns derived in the multivariate analysis (notably the relatively decreased binding in caudate in SPDRP and relatively increased binding in hypothalamus and hippocampus in LRRK2-NMC pattern). While overall consistent, the results from the univariate analysis in this work differ slightly in terms of significance from those reported in our previous publication (Wile et al., 2017) due to the involvement of a larger number of ROIs: notably the separation of the striatum region into caudate and putamen, and the addition of the substantia nigra, amygdala and hippocampus. Here the main focus was to identify subtle disease or genotype specific changes at a global network level, aiming to capture all widespread serotonergic projections instead of restricting the analysis to specific ROIs.

4.4. Comparison with other network analysis patterns

We compared SPDRP to other network patterns reported in the literature (FDG PCA-based analysis and resting-state fMRI functional connectivity analysis) to explore possible relationships between the serotonergic system, metabolic activity and resting-state functional connectivity. SPDRP did not resemble FDG PDRP, FDG PDCP or fMRI –derived patterns; this was to some degree expected given the different topology of the serotonergic network compared to the more extended brain circuitry involved in metabolic and hemodynamic activities.

4.5. Limitations

There are several limitations to this study. First, the multivariate analysis used to derive the patterns was based a relatively small sample size; however, we used five-fold cross validation and AIC to ensure the obtained pattern was generalizable to new datasets. In addition, since we found no difference in either multivariate or univariate analyses between sPD and LRRK2-PD subjects and LRRK2-PD group was not involved in deriving the pattern, the significantly higher expression of SPDRP in LRRK2-PD subjects further confirms the robustness of the pattern. Second, there was some overlaps in subject scores between groups for both patterns. This overlap is consistent with previous

findings obtained with univariate analysis, where no clear separation in DASB binding between healthy controls and early PD subjects was seen (Politis et al., 2010a, 2010b). The fact that we did see a significant group separation in early disease confirmed the higher sensitivity of the multivariate approach. Importantly, the two subjects with markedly different disease progression exhibited the lowest SPDRP expression and were classified as outliers in the correlation between SPDRP expression and disease duration, which would further support the robustness of this method and possibly suggest that the serotonergic systems may play a significant role in determining the course of the disease progression.

5. Conclusion

Using [^{11}C]-DASB PET this study provides a first evidence for the existence of a serotonergic spatial covariance pattern characteristic of PD (SPDRP) and a distinct pattern observed in subjects at increased risk of PD due to mutations in LRRK2-NMC. Even though the SPDRP was derived using sPD subjects only, a significant expression of the same covariance pattern was also observed for LRRK2-PD. The pattern was found to be strongly correlated with disease duration except for two subjects, both of whom exhibited an unusual disease course, one of them being initially characterized as a SWEDD. The pattern also correlated strongly with the putaminal dopaminergic denervation as estimated from DTBZ imaging. Compared to previously used univariate analysis approaches, the spatial covariance method was found to be more sensitive in identifying disease-related abnormalities. This finding suggests that disease-induced alterations of the serotonergic system, rather than being purely local, also affect interactions between separate regions in a disease specific fashion and is closely linked to abnormalities in the dopaminergic system. Likewise, the characteristic pattern observed in the LRRK2-NMC could provide new insights into disease mechanisms and identify either early compensatory changes or risk factors while the dopaminergic system is intact. Longitudinal observations and a larger subject cohort are required to disentangle these aspects.

Funding

The study was supported by the Canadian Institutes for Health Research (MOP-125989) and the Michael J Fox Foundation (23463). TRIUMF receives funding from the National Research Council of Canada.

Declarations of interest

None.

Acknowledgements

We are deeply grateful to all subject volunteers involved in this project for their cooperation. We thank the PET scanning staff at UBC, TRIUMF for assistance with radiotracer production and Dr. Y. Ma for sharing the analysis software. TRIUMF receives federal funding from the National Research Council of Canada.

Appendix A. Supplementary data

Supplementary data to this article can be found online at https://doi.org/10.1016/j.nicl.2018.05.022.

References

Adams, J.R., Van Netten, H., Schulzer, M., Mak, E., Mckenzie, J., Strongosky, A., Sossi, V., Ruth, T.J., Lee, C.S., Farrer, M., Gasser, T., Uitti, R.J., Calne, D.B., Wszolek, Z.K., Stoessl, A.J., 2005. PET in LRRK2 mutations: comparison to sporadic Parkinson's disease and evidence for presymptomatic compensation. Brain 128, 2777–2785. http://dx.doi.org/10.1093/brain/awh607.

Akaike, H., 1976. An information criterion (AIC). Math. Sci. 14, 5–9.

Bardien, S., Lesage, S., Brice, A., J, C., 2011. Genetic characteristics of leucine-rich repeat kinase 2 (LRRK2) associated Parkinson's disease. Parkinsonism Relat. Disord. 17, 501–508.

Braak, H., Del Tredici, K., Rüb, U., de Vos, R.A.I., Steur, E.N.H.J., Braak, E., 2003. Staging of brain pathology related to sporadic Parkinson's disease. Neurobiol. Aging 24, 197–211.

Braak, H., Ghebremedhin, E., Rüb, U., Bratzke, H., Del Tredici, K., 2004. Stages in the development of Parkinson's disease-related pathology. Cell Tissue Res. http://dx.doi.org/10.1007/s00441-004-0956-9.

Comtat, C., Bataille, F., Michel, C., Jones, J.P., Sibomana, M., Janeiro, L., Trebossen, R., 2004. OSEM-3D reconstruction strategies for the ECAT HRRT. IEEE Symp. Conf. Rec. Nucl. Sci. 2004 (6), 3492–3496. http://dx.doi.org/10.1109/NSSMIC.2004.1466639.

Dagher, A., Owen, A.M., Boecker, H., Brooks, D.J., 2001. The role of the striatum and hippocampus in planning: a PET activation study in Parkinson's disease. Brain 124, 1020–1032. http://dx.doi.org/10.1093/brain/124.5.1020.

Eckert, T., Tang, C., Eidelberg, D., 2007. Assessment of the progression of Parkinson's disease: a metabolic network approach. Lancet Neurol. http://dx.doi.org/10.1016/S1474-4422(07)70245-4.

Eidelberg, D., 2009. Metabolic brain networks in neurodegenerative disorders: a functional imaging approach. Trends Neurosci. 32, 548–557.

Gunn, R.N., Lammertsma, A.A., Hume, S.P., Cunningham, V.J., 1997. Parametric imaging of ligand-receptor binding in PET using a simplified reference region model. NeuroImage 6, 279–287.

Habeck, C., Stern, Y., Alzheimer's Disease Neuroimaging Initiative, the A.D.N, 2010. Multivariate data analysis for neuroimaging data: overview and application to Alzheimer's disease. Cell Biochem. Biophys. 58, 53–67. http://dx.doi.org/10.1007/s12013-010-9093-0.

Healy, D.G., Falchi, M., O'Sullivan, S.S., Bonifati, V., Durr, A., Bressman, S., Brice, A., Aasly, J., Zabetian, C.P., Goldwurm, S., Ferreira, J.J., Tolosa, E., Kay, D.M., Klein, C., Williams, D.R., Marras, C., Lang, A.E., Wszolek, Z.K., Berciano, J., Schapira, A.H.V., Lynch, T., Bhatia, K.P., Gasser, T., Lees, A.J., Wood, N.W., International LRRK2 Consortium, on behalf of the I.L., 2008. Phenotype, genotype, and worldwide genetic penetrance of LRRK2-associated Parkinson's disease: a case-control study. Lancet Neurol. 7, 583–590. http://dx.doi.org/10.1016/S1474-4422(08)70117-0.

Holm, S., 1979. A simple sequentially rejective multiple test procedure. Scand. J. Stat. http://dx.doi.org/10.2307/4615733.

Huang, C., Mattis, P., Tang, C., Perrine, K., Carbon, M., Eidelberg, D., 2007. Metabolic brain networks associated with cognitive function in Parkinson's disease. NeuroImage 34, 714–723. http://dx.doi.org/10.1016/j.neuroimage.2006.09.003.

Innis, R.B., Cunningham, V.J., Delforge, J., Fujita, M., Gjedde, A., Gunn, R.N., Holden, J., Houle, S., Huang, S.-C., Ichise, M., et al., 2007. Consensus nomenclature for in vivo imaging of reversibly binding radioligands. J. Cereb. Blood Flow Metab. 27, 1533–1539.

de Jong, H.W.A.M., van Velden, F.H.P., Kloet, R.W., Buijs, F.L., Boellaard, R., Lammertsma, A.A., 2007. Performance evaluation of the ECAT HRRT: an LSO-LYSO double layer high resolution, high sensitivity scanner. Phys. Med. Biol. 52, 1505–1526. http://dx.doi.org/10.1088/0031-9155/52/5/019.

Kish, S.J., Tong, J., Hornykiewicz, O., Rajput, A., Chang, L.-J.J., Guttman, M., Furukawa, Y., 2008. Preferential loss of serotonin markers in caudate versus putamen in Parkinson's disease. Brain 131, 120–131. http://dx.doi.org/10.1093/brain/awm239.

de Lau, L.M.L., Breteler, M.M.B., 2006. Epidemiology of Parkinson's disease. Lancet Neurol. 5, 525–535.

Liu, S.Y., Wile, D.J., Fu, J.F., Valerio, J., Shahinfard, E., McCormick, S., Mabrouk, R., Vafai, N., McKenzie, J., Neilson, N., Perez-Soriano, A., Arena, J.E., Cherkasova, M., Chan, P., Zhang, J., Zabetian, C.P., Aasly, J.O., Wszolek, Z.K., McKeown, M.J., Adam, M.J., Ruth, T.J., Schulzer, M., Sossi, V., Stoessl, A.J., 2018. The effect of LRRK2 mutations on the cholinergic system in manifest and premanifest stages of Parkinson's disease: a cross-sectional PET study. Lancet Neurol. 17, 309–316. http://dx.doi.org/10.1016/S1474-4422(18)30032-2.

Loane, C., Wu, K., Bain, P., Brooks, D.J., Piccini, P., Politis, M., 2013. Serotonergic loss in motor circuitries correlates with severity of action-postural tremor in PD. Neurology 80, 1850–1855. http://dx.doi.org/10.1212/WNL.0b013e318292a31d.

Lozza, C., Baron, J.-C.C., Eidelberg, D., Mentis, M.J., Carbon, M., Marié, R.-M.M., 2004. Executive processes in Parkinson's disease: FDG-PET and network analysis. Hum. Brain Mapp. 22, 236–245. http://dx.doi.org/10.1002/hbm.20033.

Marder, K., Wang, Y., Alcalay, R.N., Mejia-Santana, H., Tang, M.-X., Lee, A., Raymond, D., Mirelman, A., Saunders-Pullman, R., Clark, L., Ozelius, L., Orr-Urtreger, A., Giladi, N., Bressman, S., LRRK2 Ashkenazi Jewish Consortium, F. The L.A.J, Alcalay, R.N., Tang, M.-X., Santana, H.M., Roos, E., Orbe-Reilly, M., Fahn, S., Cote, L., Waters, C., Mazzoni, P., Ford, B., Louis, E., Levy, O., Rosado, L., Ruiz, D., Dorovski, T., Greene, P., Clark, L., Marder, K.S., Gurevich, T., Shira, A.B., Weisz, M.G., Yasinovsky, K., Zalis, M., Thaler, A., Balash, Y., Hertzel, S., Or, Z.G., Kobo, H., Hillel, A., Shkedy, A., Orr-Urtreger, A., Giladi, N., Deik, A., Barrett, M.J., Cabassa, J., Groves, M., Hunt, A.L., Lubarr, N., Luciano, M.S., Miravite, J., Palmese, C., Sachdev, R., Sarva, H., Severt, L., Shanker, V., Swan, M.C., Soto-Valencia, J., Johannes, B., Ortega, R., Ozelius, L., Saunders-Pullman, R., Raymond, D., Bressman, S., 2015. Age-specific penetrance of LRRK2 G2019S in the Michael J. Fox Ashkenazi Jewish LRRK2 consortium. Neurology 85, 89–95. http://dx.doi.org/10.1212/WNL.0000000000001708.

Marras, C., Schuele, B., Munhoz, R.P., Rogaeva, E., Langston, J.W., Kasten, M., Meaney, C., Klein, C., Wadia, P.M., Lim, S.Y., Chuang, R.S.I., Zadikof, C., Steeves, T., Prakash, K.M., De Bie, R.M.A., Adeli, G., Thomsen, T., Johansen, K.K., Teive, H.A., Asante, A., Reginold, W., Lang, A.E., 2011. Phenotype in parkinsonian and nonparkinsonian

LRRK2 G2019S mutation carriers. Neurology 77, 325–333. http://dx.doi.org/10.1212/WNL.0b013e318227042d.

Marras, C., Alcalay, R.N., Caspell-Garcia, C., Coffey, C., Chan, P., Duda, J.E., Facheris, M.F., Fernández-Santiago, R., Ruíz-Martínez, J., Mestre, T., Saunders-Pullman, R., Pont-Sunyer, C., Tolosa, E., Waro, B., 2016. Motor and nonmotor heterogeneity of LRRK2-related and idiopathic Parkinson's disease. Mov. Disord. 31, 1192–1202. http://dx.doi.org/10.1002/mds.26614.

Meyer, J.H., Wilson, A.A., Ginovart, N., Goulding, V., Hussey, D., Hood, K., Houle, S., 2001. Occupancy of serotonin transporters by paroxetine and citalopram during treatment of depression: a [C-11]DASB PET imaging study. Am. J. Psychiatry 158, 1843–1849. http://dx.doi.org/10.1176/appi.ajp.158.11.1843.

Nandhagopal, R., Mak, E., Schulzer, M., McKenzie, J., McCormick, S., Sossi, V., Ruth, T.J., Strongosky, A., Farrer, M.J., Wszolek, Z.K., Stoessl, A.J., 2008. Progression of dopaminergic dysfunction in a LRRK2 kindred: a multitracer PET study. Neurology 71, 1790–1795. http://dx.doi.org/10.1212/01.wnl.0000335973.66333.58.

Ouchi, Y., Yoshikawa, E., Okada, H., Futatsubashi, M., Sekine, Y., Iyo, M., Sakamoto, M., 1999. Alterations in binding site density of dopamine transporter in the striatum, orbitofrontal cortex, and amygdala in early Parkinson's disease: compartment analysis for [11C]-CFT binding with positron emission tomography. Ann. Neurol. 45, 601–610(https://doi.org/10.1002/1531-8249(199905)45:5 < 601::AID-ANA8 > 3.0.CO;2-0).

Politis, M., Loane, C., 2011. Serotonergic dysfunction in Parkinson's disease and its relevance to disability. Sci. World J. 11, 1726–1734. http://dx.doi.org/10.1100/2011/172893.

Politis, M., Wu, K., Loane, C., Kiferle, L., Molloy, S., Brooks, D.J., Piccini, P., 2010a. Staging of serotonergic dysfunction in Parkinson's disease: an in vivo 11 C-DASB PET study. Neurobiol. Dis. 40, 216–221.

Politis, M., Wu, K., Loane, C., Turkheimer, F.E., Molloy, S., Brooks, D.J., Piccini, P., 2010b. Depressive symptoms in PD correlate with higher 5-HTT binding in raphe and limbic structures. Neurology 75, 1920–1927.

Politis, M., Loane, C., Wu, K., Brooks, D.J., Piccini, P., 2011. Serotonergic mediated body mass index changes in Parkinson's disease. Neurobiol. Dis. 43, 609–615.

Scholtissen, B., Verhey, F.R.J., Steinbusch, H.W.M., Leentjens, A.F.G., 2006. Serotonergic mechanisms in Parkinson's disease: opposing results from preclinical and clinical data. J. Neural Transm. 113, 59–73. http://dx.doi.org/10.1007/s00702-005-0368-3.

Schrag, A., Horsfall, L., Walters, K., Noyce, A., Petersen, I., 2015. Prediagnostic presentations of Parkinson's disease in primary care: a case-control study. Lancet Neurol. 14, 57–64. http://dx.doi.org/10.1016/S1474-4422(14)70287-X.

Sierra, M., Sánchez-Juan, P., Martínez-Rodríguez, M.I., González-Aramburu, I., García-Gorostiaga, I., Quirce, M.R., Palacio, E., Carril, J.M., Berciano, J., Combarros, O., Infante, J., 2013. Olfaction and imaging biomarkers in premotor LRRK2 G2019S-associated Parkinson disease. Neurology 80, 621–626. http://dx.doi.org/10.1212/WNL.0b013e31828250d6.

Sossi, V., de la Fuente-Fernández, R., Nandhagopal, R., Schulzer, M., McKenzie, J., Ruth, T.J., Aasly, J.O., Farrer, M.J., Wszolek, Z.K., Stoessl, J.A., 2010. Dopamine turnover increases in asymptomatic LRRK2 mutations carriers. Mov. Disord. 25, 2717–2723. http://dx.doi.org/10.1002/mds.23356.

Srivatsal, S., Cholerton, B., Leverenz, J.B., Wszolek, Z.K., Uitti, R.J., Dickson, D.W., Weintraub, D., Trojanowski, J.Q., Van Deerlin, V.M., Quinn, J.F., Chung, K.A., Peterson, A.L., Factor, S.A., Wood-Siverio, C., Goldman, J.G., Stebbins, G.T., Bernard, B., Ritz, B., Rausch, R., Espay, A.J., Revilla, F.J., Devoto, J., Rosenthal, L.S., Dawson, T.M., Albert, M.S., Mata, I.F., Hu, S.C., Montine, K.S., Johnson, C., Montine, T.J., Edwards, K.L., Zhang, J., Zabetian, C.P., 2015. Cognitive profile of LRRK2-related Parkinson's disease. Mov. Disord. 30, 728–733. http://dx.doi.org/10.1002/mds.26161.

Stoessl, A.J., 2009. Functional imaging studies of non-motoric manifestations of Parkinson's disease. Parkinsonism Relat. Disord. 15, S13–S16. http://dx.doi.org/10.1016/S1353-8020(09)70771-0.

Stoessl, A.J., Vaillancourt, D., Spraker, M., Prodoehl, J., Abraham, I., Corcos, D., Zhou, X., Al, E., Peran, P., Cherubini, A., Assogna, F., Piras, F., Quattrocchi, C., Peppe, A., Takeda, A., Saito, N., Baba, T., Kikuchi, A., Sugeno, N., Kobayashi, M., Al, E., Bohnen, N., Muller, M., Kotagal, V., Koeppe, R.M.M., Kilbourn, M., Albin, R., Al, E., Boileau, I., Warsh, J., Guttman, M., Saint-Cyr, J., McCluskey, T., Rusjan, P., Al, E., Albin, R., Koeppe, R.M.M., Bohnen, N., Wernette, K., Kilbourn, M., Frey, K., Albin, R., Koeppe, R.M.M., Chervin, R., Consens, F., Wernette, K., Frey, K., Al, E., Iranzo, A., Valldeoriola, F., Lomena, F., Molinuevo, J., Serradell, M., Salamero, M., Al, E., Unger, M., Belke, M., Menzler, K., Heverhagen, J., Keil, B., Stiasny-Kolster, K., Al, E., Kashihara, K., Imamura, T., Shinya, T., Antonini, A., Leenders, K., Vontobel, P., Maguire, R., Missimer, J., Psylla, M., Al, E., Yoshita, M., Ma, Y., Huang, C., Dyke, J., Pan, H., Alsop, D., Feigin, A., Al, E., Tang, C., Poston, K., Eckert, T., Feigin, A., Frucht, S., Gudesblatt, M., Al, E., Sossi, V., de la Fuente-Fernandez, R., Nandhagopal, R., Schulzer, M., McKenzie, J., Ruth, T., Al, E., Khan, N., Scherfler, C., Graham, E., Bhatia, K., Quinn, N., Lees, A., Al, E., Khan, N., Valente, E., Bentivoglio, A., Wood, N., Albanese, A., Brooks, D., Al, E., Vingerhoets, F., Schulzer, M., Calne, D., Snow, B., Doder, M., Rabiner, E., Turjanski, N., Lees, A., Brooks, D., Nandhagopal, R., Kuramoto, L., Schulzer, M., Mak, E., Cragg, J.K.L., Lee, C., Al, E., de la Fuente-Fernandez, R., Schulzer, M., Cragg, J.K.L., Ramachandiran, N., Au, W., Al, E., Huang, C., Tang, C., Feigin, A., Lesser, M., Ma, Y., Pourfar, M., Al, E., Martin, W., Wieler, M., Gee, M., Gerhard, A., Pavese, N., Hotton, G., Turkheimer, F., Es, M., Hammers, A., Al, E., Ouchi, Y., Yoshikawa, E., Sekine, Y., Futatsubashi, M., Kanno, T., Ogusu, T., Al, E., Miyoshi, M., Shinotoh, H., Wszolek, Z., Strongosky, A., Shimada, H., Arakawa, R., Al, E., Bohnen, N., Koeppe, R.M.M., Studenski, S., Kilbourn, M., Frey, K., Al, E., Maetzler, W., Liepelt, I., Reimold, M., Reischl, G., Solbach, C., Becker, C., Al, E., Jokinen, P., Scheinin, N., Aalto, S., Nagren, K., Savisto, N., Parkkola, R., Al, E., Claassen, D., Lowe, V., Peller, P., Petersen, R., Josephs, K., 2012. Neuroimaging in Parkinson's disease: from pathology to diagnosis. Parkinsonism Relat. Disord. 18 (Suppl. 1), S55–S59. http://dx.doi.org/10.1016/S1353-8020(11)70019-0.

Tessitore, A., Hariri, A.R., Fera, F., Smith, W.G., Chase, T.N., Hyde, T.M., Weinberger, D.R., Mattay, V.S., 2002. Dopamine modulates the response of the human amygdala: a study in Parkinson's disease. J. Neurosci. 22, 9099–9103(https://doi.org/12388617).

Trinh, J., Gustavsson, E.K., Vilariño-Güell, C., Bortnick, S., Latourelle, J., McKenzie, M.B., Tu, C.S., Nosova, E., Khinda, J., Milnerwood, A., Lesage, S., Brice, A., Tazir, M., Aasly, J.O., Parkkinen, L., Haytural, H., Foroud, T., Myers, R.H., Sassi, S. Ben, Hentati, E., Nabli, F., Farhat, E., Amouri, R., Hentati, F., Farrer, M.J., 2016. DNM3 and genetic modifiers of age of onset in LRRK2 Gly2019Ser parkinsonism: a genome-wide linkage and association study. Lancet Neurol. 15, 1248–1256. http://dx.doi.org/10.1016/S1474-4422(16)30203-4.

Wile, D.J., Dinelle, K., Vafai, N., McKenzie, J., Tsui, J.K., Schaffer, P., Ding, Y.S., Farrer, M., Sossi, V., Stoessl, A.J., 2016. A scan without evidence is not evidence of absence: scans without evidence of dopaminergic deficit in a symptomatic leucine-rich repeat kinase 2 mutation carrier. Mov. Disord. 31, 405–409. http://dx.doi.org/10.1002/mds.26450.

Wile, D.J., Agarwal, P.A., Schulzer, M., Mak, E., Dinelle, K., Shahinfard, E., Vafai, N., Hasegawa, K., Zhang, J., McKenzie, J., Neilson, N., Strongosky, A., Uitti, R.J., Guttman, M., Zabetian, C.P., Ding, Y.-S., Adam, M., Aasly, J., Wszolek, Z.K., Farrer, M., Sossi, V., Stoessl, A.J., 2017. Serotonin and dopamine transporter PET changes in the premotor phase of LRRK2 Parkinsonism: cross-sectional studies. Lancet Neurol. 16, 351–359. http://dx.doi.org/10.1016/S1474-4422(17)30056-X.

Wu, Y., Carson, R.E., 2002. Noise reduction in the simplified reference tissue model for neuroreceptor functional imaging. J. Cereb. Blood Flow Metab. 22, 1440–1452. http://dx.doi.org/10.1097/01.WCB.0000033967.83623.34.